Thalamo-cortical coupling during encoding and consolidation is linked to durable memory formation

Wagner, Isabella C.; van Buuren, Mariët; Fernández, Guillén

published in
NeuroImage
2019

DOI (link to publisher)
10.1016/j.neuroimage.2019.04.055

document version
Publisher's PDF, also known as Version of record

NeuroImage 197 (2019) 80–92

Contents lists available at ScienceDirect

NeuroImage

journal homepage: www.elsevier.com/locate/neuroimage

Thalamo-cortical coupling during encoding and consolidation is linked to durable memory formation

Isabella C. Wagner [a,b,*], Mariët van Buuren [a,c], Guillén Fernández [a]

[a] Donders Institute for Brain, Cognition and Behaviour, Radboud University Nijmegen Medical Center, Nijmegen, 6525 EZ, The Netherlands
[b] Social, Cognitive and Affective Neuroscience Unit, Department of Basic Psychological Research and Research Methods, Faculty of Psychology, University of Vienna, Liebiggasse 5, 1010, Vienna, Austria
[c] Department of Clinical, Neuro and Developmental Psychology, Faculty of Behavioral and Movement Sciences, Institute for Brain and Behavior Amsterdam, Vrije Universiteit Amsterdam, Van der Boechorststraat 7, 1081 BT, Amsterdam, The Netherlands

ARTICLE INFO

Keywords:
Medioventral thalamus
Durable memory
Consolidation
Connectivity
Resting-state
fMRI

ABSTRACT

Memory formation transforms experiences into durable engrams. The stabilization critically depends on processes during and after learning, and involves hippocampal-medial prefrontal interactions that appear to be mediated by the nucleus reuniens of the thalamus in rodents, which corresponds to the human medioventral thalamus. How this region contributes to durable memory formation in humans is, however, unclear. Furthermore, the anterior-, lateral dorsal-, and mediodorsal nuclei appear to promote mnemonic function as well. We hypothesized that durable memory formation is associated with increases in thalamo-cortical interactions during encoding and consolidation. Thirty-three human subjects underwent fMRI while studying picture-location associations. To assess consolidation, resting-state brain activity was measured after study and was compared to a pre-study baseline. Memory was tested on the same day and 48 h later. While "weak" memories could only be remembered at the immediate test, "durable" memories persisted also after the delay. We found increased coupling of the medioventral-, adjacent anterior-, lateral dorsal-, and mediodorsal thalamus with the hippocampus and surrounding medial temporal lobe, as well as with anterior and posterior midline regions related to durable memory encoding. The medioventral and lateral dorsal thalamus showed increased connectivity with posterior medial and parietal cortex from baseline to post-encoding rest, positively scaling with the proportion of durable memories formed across subjects. Additionally, the lateral dorsal thalamus revealed consolidation-related coupling with the inferior temporal, retrosplenial, and medial prefrontal cortex. We suggest that thalamo-cortical cross-talk strengthens mnemonic representations at initial encoding, and that cortical coupling of specific thalamic subregions supports consolidation thereafter.

1. Introduction

Memory formation transforms fragile representations into durable engrams (Dudai, 2004; Squire et al., 2015). While some memories decay rapidly, others are stabilized and become gradually integrated within a wider neocortical network (Marr, 1970; Frankland and Bontempi, 2005). This entails hippocampal-neocortical interactions during memory encoding (Sneve et al., 2015), as well as consolidation during sleep (Diekelmann and Born, 2010; Stickgold and Walker, 2013; Maingret et al., 2016) and awake rest (Peigneux et al., 2006; Tambini et al., 2010; van Kesteren et al., 2010). Eventually, the medial prefrontal cortex (MPFC) seems to take over the binding function of the hippocampus, linking together different mnemonic features that are stored in specific posterior representational regions (Frankland and Bontempi, 2005; Takashima et al., 2006).

While direct anatomical pathways from the hippocampus to the MPFC are unidirectional (Jay et al., 1989; Vertes, 2004; Hoover and Vertes, 2007), tracing studies in rodents showed that the nucleus reuniens of the midline thalamus (which corresponds to the medioventral thalamus in humans) exhibits connections to both the hippocampus (Dolleman-Van Der Weel and Witter, 1996) and the MPFC (Vertes, 2002, 2006; Johansen-Berg et al., 2005; Vertes et al., 2007; Hoover and Vertes, 2012; Varela et al., 2014), as well as to posterior representational regions (for a review, see Cassel et al., 2013). Thus, the

* Corresponding author. Social, Cognitive and Affective Neuroscience Unit, Department of Basic Psychological Research and Research Methods, Faculty of Psychology, University of Vienna, Liebiggasse 5, 1010, Vienna, Austria.
E-mail address: isabella.wagner@univie.ac.at (I.C. Wagner).

https://doi.org/10.1016/j.neuroimage.2019.04.055
Received 12 March 2019; Accepted 19 April 2019
Available online 24 April 2019

rat nucleus reuniens (i.e., the human medioventral thalamus) appears to be in a position to relay information between these structures and it therefore possibly also plays a role in mnemonic functioning. Studies with rodents indeed revealed that the nucleus reuniens is associated with memory specificity and generalization at encoding (Xu and Südhof, 2013), spatial processing (Cholvin et al., 2017) and memory persistence (Loureiro et al., 2012), as well as with memory consolidation after learning (Davoodi et al., 2011). Furthermore, Barker and Warburton (2018) recently demonstrated that lesions of the rat nucleus reuniens impaired long-term, but not short term associative recognition memory formation (Barker and Warburton, 2018). Thus, the nucleus reuniens appears involved in durable memory formation during encoding and consolidation in rodents. We hypothesized a similar role of the corresponding medioventral thalamus in humans.

Several other thalamic nuclei have been associated with mnemonic function. The anterior thalamus (i.e., the anterior dorsal, -medial, and -ventral thalamus) was previously linked to general memory formation (Sweeney-Reed et al., 2014, 2015, 2016), retrieval (Pergola et al., 2013), and attention-guided mnemonic processing (Wright et al., 2015; Leszczyński and Staudigl, 2016). Rodent work implicates the anterior- (Taube, 1995; Aggleton et al., 1996; Aggleton and Brown, 1999; Aggleton and Nelson, 2015), as well as the adjacent lateral dorsal thalamus in spatial processing and memory (Mizumori and Williams, 1993; Mizumori et al., 1994; Warburton et al., 1997; van Groen et al., 2002). The mediodorsal thalamus (i.e., magnocellular and parvocellular nuclei) was related to memory formation (Mitchell and Gaffan, 2008; Pergola et al., 2013; Sweeney-Reed et al., 2016) and associative memory (Cross et al., 2012; Pergola et al., 2013), and is known to densely project to the prefrontal cortex to support general cognition (Klein et al., 2010; Parnaudeau et al., 2013, 2015; Browning et al., 2015; Miller et al., 2017). Although there are no direct structural connections between mediodorsal thalamus and hippocampus (Vertes, 2004), it is thought to contribute to memory via an extrahippocampal circuit (Ketz et al., 2015). Overall, along with the medioventral thalamus, the anterior-, lateral dorsal-, and mediodorsal thalamus seem relevant for memory processing, encoding in particular. Here, we asked how these four thalamic regions contribute to different aspects of durable memory formation in humans.

Human subjects underwent functional MRI while intentionally encoding picture-location associations (Fig. 1AB; see also Wagner et al., 2016). Neural activity related to consolidation was assessed during rest periods after encoding by comparing to baseline rest activity acquired before study. To capture durable memories, study material was tested on the same day and 48 h later (Fig. 1A). While "weak" memories could only be remembered at the immediate test, "durable" memories persisted also after 48 h. First, we hypothesized that increased thalamo-cortical connectivity of the medioventral-, anterior-, lateral dorsal-, and mediodorsal thalamus would be associated with durable memory formation at encoding. Due to the small size of the medioventral thalamus, we combined it with the adjacent central medial nucleus to form an enlarged region and refer to it as medioventral thalamus^{+}. Second, we hypothesized thalamic connectivity increases, in particular of the medioventral thalamus^{+}, from baseline to post-encoding rest to be positively related to individual variations in memory durability. This should entail consolidation-related coupling with posterior representational regions that are also involved during encoding (Tambini et al., 2010; van Kesteren et al., 2010; Schlichting and Preston, 2014). We expected engagement of the inferior temporal and posterior parietal cortex since these regions likely coded for picture content (Martin et al., 1996; Kriegeskorte et al., 2008; Grill-Spector and Weiner, 2014) and different picture locations (Burgess et al., 2001; Sereno et al., 2001; Takashima et al., 2007) of the studied associations, respectively.

2. Materials and methods

2.1. Subjects

Thirty-five subjects participated in this experiment (23 females, age range = 18–29 years, mean = 23). All subjects were right-handed, healthy, had normal or corrected-to-normal vision, and gave written informed consent prior to participation. We excluded one subject due to technical problems with the MR gradient coil, and one subject due to technical failure of the cardiorespiratory recordings. Final analyses included 33 subjects (23 females, age range = 18–29 years, mean = 23). The study was approved by the institutional review board (Comissie Mensgebonden Onderzoek, Arnhem-Nijmegen, The Netherlands).

2.2. Experimental design and associative memory task

Subjects studied a total of 192 picture-location associations (study phase) that were distributed over two cycles. Resting-state periods were

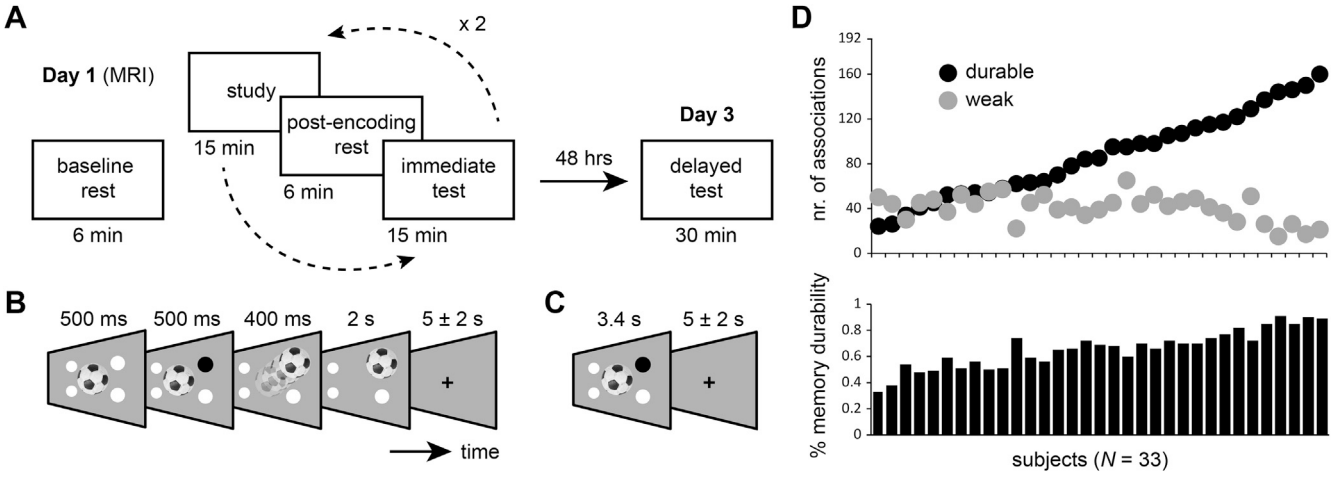

Fig. 1. Study timeline, associative memory task, and memory performance. **(A)** Subjects studied 192 unique picture-location associations and were tested for their immediate memory (immediate test, day 1) during two study-rest-test cylces (schematically indicated with dashed arrows), and during a delayed memory test 48 h later (delayed test, day 3). Subjects were scanned during an initial baseline resting-state period, as well as during resting-state periods after the study phase of each of the two cycles (post-encoding rest). **(B)** During study trials, pictures were randomly associated with one of four locations and subjects were instructed to intentionally encode the associations. **(C)** During immediate and delayed tests, the picture was presented centrally and subjects were required to indicate the correct location by pressing one of four buttons (example response marked in black). **(D) Upper part:** Distribution of durable and weak memories across subjects. **Lower part:** Distribution of memory durability scores across subjects (see also Section 2.3.).

placed before the study phase (baseline rest), and after study within each cycle (post-encoding rest; see Section 2.4). Picture-location associations were retrieved following the post-encoding rest periods (immediate test, day 1), as well as 48 h later (delayed test, day 3; Fig. 1A). Thus, subjects completed one baseline rest and two study-rest-test cycles while undergoing fMRI, as well as one delayed test outside the scanner.

During the study phase of each study-rest-test cycle (2×15 min), subjects memorized 96 sequentially presented, colored photographs (e.g., animals, plants, objects, buildings; 24 pictures each) that were randomly associated with one of four screen locations (lower left, upper left, lower right, upper right; similar to Takashima et al., 2009; van Dongen et al., 2011, 2012). A trial started with the presentation of a picture in the center of the screen (1 s) together with the four surrounding screen locations as filled white circles. After 500 ms, one of the filled circles turned green indicating the target location of the respective picture. The picture then moved to that target location (400 ms) and remained there for 2 s. Inter-trial-intervals varied randomly between 3 and 7 s (mean = 5 s) during which a fixation cross was presented (Fig. 1B). Subjects were provided with a break of 25 s every 32 trials indicated by asterisks on the computer screen.

At the immediate test of each study-rest-test cycle (2×15 min), subjects were prompted for their memory of all picture-location associations that were shown during the preceding cycle (i.e., 96 trials). Again, pictures were presented in the center of the screen surrounded by the four filled white circles indicating the potential screen locations (3.4 s; Fig. 1C). Subjects were required to press one of four buttons using their middle and index fingers (i.e., one button box in each hand, two buttons per box, each topographically mapped to upper and lower screen locations). Trials were separated by a fixation period ranging between 3 and 7 s (mean = 5 s) and a break of 25 s was given every 32 trials. The delayed test was performed in front of a computer screen in a behavioral laboratory on day 3 (mean delay = 47 h; range = 45–50 h). Timing and structure were identical to the immediate test (day 1) but all 192 picture-location associations were randomly presented within one cycle (30 min). The experiment was programmed and presented with Presentation (version 16.4, www.neurobs.com).

2.3. Behavioral data and memory durability scores

Trials were sorted based on the subjects' performance at the immediate (day 1) and the delayed test (day 3). This resulted in three types of responses: picture-location associations that were (1) already forgotten on day 1 ("forgotten"); (2) remembered on day 1 but forgotten on day 3 ("weak"); or (3) remembered at both tests ("durable"). Picture-location associations that were forgotten at the immediate test (day 1) but recalled correctly at the delayed test (day 3; mean ± SEM: 16 ± 1.3 trials) were regarded as guesses (forgotten ∩ forgotten-remembered: 60 ± 5.4 trials; 60/4 locations, chance-level = 15; $p = 0.594$) and were grouped together with associations that were forgotten at both tests (day 1 and 3). Subjects only displayed very few trials with no responses ("misses"; 3 ± 1 trials across both days).

As part of our analyses, we aimed at identifying connectivity profiles during resting-state that were associated with durable memory consolidation. Specifically, we reasoned that consolidation processes during post-encoding rest would be more pronounced for durable than for weak memories. To this end, we calculated a behavioral "memory durability score" for each subject. We divided the number of durable associations by the total number of remembered associations (durable ∩ weak; i.e. the proportion of durable memories), thereby normalizing individual memory durability scores for general memory performance. These scores were used as a covariate of interest for resting-state connectivity analysis (see Section 2.7.5.). To determine whether our alleged effects were not only associated with durable but also with general memory performance, we further calculated a "general memory performance score" per subject, dividing the number of remembered associations by the total number of associations (remembered ∩ forgotten; i.e., the proportion of remembered associations). As above, these scores were included as a covariate of interest in our resting-state connectivity analysis.

2.4. Resting-state periods

Subjects were scanned during three 6-min resting-state periods. A first baseline rest was recorded before the start of the study phase of the associative memory task (baseline rest; see Section 2.2.; Fig. 1A). To assess intrinsic connectivity changes related to durable memory consolidation after encoding, rest periods were placed after the study phase of each study-rest-test cycle (post-encoding rest). Subjects were instructed to remain awake with their eyes open while a white fixation cross was presented at the center of the computer screen. Compliance was verified with eye tracking. All recordings were visually inspected and it was secured that subjects kept their eyes open (except for eye blinks), and that they fixated the screen throughout the task, indicating attentive processing.

2.5. Cardiorespiratory recordings and preprocessing

During resting-state, cardiorespiratory signals were shown to resonate in the same frequency band (~0.03–0.1 Hz) as the low-frequency fluctuations of interest in the blood-oxygen-level-dependent (BOLD) signal (0.01–0.1 Hz; Birn et al., 2006; Shmueli et al., 2007; van Buuren et al., 2009). Therefore, to account for the impact of these confounding signals on resting-state connectivity, we recorded heart rate (HR; i.e. finger pulse) and respiration during MRI data acquisition. HR was measured with a pulse oximeter affixed to the little finger of the right hand, and respiration was measured with a respiration belt placed around the subjects' abdomen. Data was recorded with a MR-compatible BrainAmp MR amplifier (Brainproducts, Munich, Germany) and digitized at a sampling rate of 5000 Hz. Data recordings as well as storage were controlled using the Brain Vision Recorder (Brainproducts). The raw signal was visually inspected for R-peaks and corrected for artifacts. To correct the resting-state BOLD fMRI data for cardiorespiratory effects, we used RETROICOR (20 regressors; Glover et al., 2000) and additional time-delayed regressors for HR and respiration volume per unit time, shifted with 6, 10, and 12 s, and −1 and 5 s, respectively (5 regressors; Birn et al., 2006; Shmueli et al., 2007; van Buuren et al., 2009).

2.6. MRI data acquisition

Imaging data were acquired using a 3 T MRI scanner (Skyra, Siemens, Erlangen, Germany) equipped with a 32-channel head coil. We obtained 405 T_2*-weighted BOLD images during study and immediate test phases of each cycle, as well as 172 T_2*-weighted BOLD images during the three resting-state periods (baseline rest, 2 × post-encoding rest), using a gradient multi-echo EPI sequence. The application of multiple echo times (TEs) was shown to increase the signal-to-noise ratio because it allows region-specific TEs (Poser et al., 2006). For instance, signal from the medial temporal lobe (MTL) and the MPFC benefits from shorter TEs, given the neighboring air-filled cavities. Signal from other brain regions, like areas at the convexity, yield an optimal BOLD contrast at longer TEs. Parameters were as follows: TR = 2180 ms, TEs = 7.5, 18.3, 29, 40 ms, flip angle = 90°, FOV = 224 × 224 mm, matrix = 74 × 74, 34 ascending axial slices, 21% slice gap, voxel size = 3 mm isotropic. Structural scans were acquired using a Magnetization-Prepared Rapid Gradient Echo (MP-RAGE) sequence with the following parameters: TR = 2300 ms, TE = 3.03 ms, flip angle = 8°, FOV = 256 × 256 mm, voxel size = 1 mm isotropic.

2.7. Data processing and statistical analysis

2.7.1. MRI data preprocessing

All imaging data were analyzed using SPM8 (http://www.fil.ion.ucl.ac.uk/spm/) in combination with Matlab (version 2012b, The

Mathworks, Natick, MA, USA). As a first step, echoes from the four different echo-times were combined into single volumes (Poser et al., 2006; van Buuren et al., 2014; Wagner et al., 2015, 2016, 2017). We used 56 scans that were acquired during a short resting-state period (2 min) before the start of the baseline rest to determine the optimal weighting of echo-times for each voxel. This was done by calculating the contrast-to-noise ratio for each echo per scan. Images from multiple echo-times were then combined by performing motion correction on the first echo, estimating iterative rigid body realignment to minimize the residual sum of squares between the first echo of the first scan and all remaining scans. The estimated parameters were then applied to all other echoes, realigning all echoes to the first echo of the first scan. Finally, the calculated optimal echo-time weightings were used to combine the four echo images into a single image. These combined images were used for all further preprocessing and analyses.

The first six volumes were discarded to allow for T1-equilibration. The combined EPI-volumes were then slice time corrected to the middle slice and realigned to the mean image of both cycles. The structural scan was co-registered to the mean functional scan and segmented into grey matter, white matter and cerebrospinal fluid using the "New Segmentation" algorithm. All images (functional and structural) were spatially normalized to the Montreal Neurological Institute (MNI) EPI template using Diffeomorphic Anatomical Registration Through Exponentiated Lie Algebra (DARTEL; Ashburner, 2007), and functional images were further smoothed with a 3D Gaussian kernel (6 mm full-width at half maximum, FWHM).

Additionally, we used multiple linear regression to correct for cardiorespiratory effects, motion, and low-frequency signal-drifts in the resting-state data. The regression model included the 25 regressors capturing cardiorespiratory effects (see Section 2.5.), and the 6 realignment parameters. Further, we removed scans affected by head motion using "motion scrubbing" (Power et al., 2012). We calculated the frame-wise displacement (*FD*) for every scan at time *t* by $FD(t) = |\Delta d_x(t)| + |\Delta d_y(t)| + |\Delta d_z(t)| + r|\alpha(t)| + r|\beta(t)| + r|\gamma(t)|$, where (dx, dy, dz) is the translational-, and (α, β, γ) the rotational movement. Scans that exceeded the head motion limit of $FD(t) > 0.3$ mm were removed (on average ~1% of the scans), indicated in one additional regressor per removed scan. Additionally, we applied a high-pass filter with a cut-off at 128 s. All resting-state connectivity analyses were performed on the residual data.

2.7.2. fMRI data modeling

Subsequent memory effects during encoding and retrieval were previously investigated by testing activation changes and representational pattern similarity (Wagner et al., 2016). Here, we predicted that thalamo-cortical interactions during encoding and consolidation would promote durable memory formation. Data during study phases of both cycles were modeled as described before (Wagner et al., 2016). In brief, trials were sorted based on individual memory performance (forgotten, weak, durable; see Section 2.3). The BOLD response was modeled with separate regressors that were time-locked to trial onset. Guesses and missed responses were combined within a task regressor for forgotten trials (see Section 2.3). Events were estimated as a boxcar function with the duration of one trial (3.4 s) and were convolved with a canonical hemodynamic response function. To account for noise due to head movement, the six realignment parameters, their first derivatives, as well as the squared first derivatives were included in the design matrix. A high-pass filter with a cutoff at 128 s was applied. Study phases of both cycles were combined into one first-level model, and task regressors were contrasted against the implicit baseline.

2.7.3. Thalamic regions-of-interest

To delineate the thalamic regions-of-interest (ROIs), we used the stereotactic mean anatomical atlas provided by Krauth and colleagues (Krauth et al., 2010) (© University of Zurich and ETH Zurich, Axel Krauth, Rémi Blanc, Alejandra Poveda, Daniel Jeanmonod, Anne Morel, Gábor Székely), which is based on histological, cytoarchitectual features defined *ex vivo* (Morel, 2007). We specified the medioventral thalamus using the medioventral nucleus mask of the stereotactic mean anatomical atlas. Due to its small size, we combined the medioventral nucleus mask with the adjacent central medial nucleus (Fig. 2A, marked in blue). To indicate that the ROI incorporated both the medioventral thalamus plus the central medial nucleus, we will refer to it as medioventral thalamus^{+}. We delineated the anterior thalamus by combining the anterior dorsal, -medial, and -ventral nucleus masks (Fig. 2A, marked in cyan). Due to its structural connections, the lateral dorsal thalamus is often, but not always, grouped together with the anterior thalamus (Puelles et al., 2012). To test the specific contributions of the lateral dorsal thalamus to durable memory processing we defined this region separately using the lateral dorsal nucleus mask (Fig. 2A, marked in red). The mediodorsal thalamus was demarcated by combining the magnocellular and parvocellular thalamic nucleus masks (Fig. 2A, marked in yellow).

Since we did not have specific hypotheses regarding the laterality of brain effects, we collapsed left and right ROIs into bilateral binary masks, using an intensity threshold of 0.25. Thalamic ROIs were then resliced to match the dimension of the functional images (medioventral thalamus^{+}, 14 voxels; anterior thalamus, 39 voxels; lateral dorsal thalamus, 18 voxels; mediodorsal thalamus, 110 voxels), and quality was confirmed through visual inspection of each seed's overlap with the individual structural and functional data in MNI standard space.

2.7.4. Connectivity during memory encoding

First, we applied Psychophysiological Interaction analysis (PPI; Friston et al., 1997) to probe functional connectivity during memory encoding. Two PPI analyses were performed per seed region to target durable, as well as general memory encoding (contrasts durable > weak, and remembered > forgotten, respectively). For each thalamic ROI, i.e. seed, the first eigenvector of the time course was extracted (i.e., the physiological factor) and adjusted for average activation during the task using an *F*-contrast. This time course was then convolved with the respective task condition (i.e., the psychological factor), and connectivity positively related to this interaction was investigated. To test for group effects, individual contrast images were submitted to one-sample *t*-tests.

For all analyses, significance was assessed using cluster-inference with a cluster-defining threshold of $p < 0.001$ and a cluster-probability of $p < 0.05$ family-wise error (FWE) corrected for multiple comparisons. The corrected cluster size threshold (i.e., the spatial extent of a cluster that is required in order to be labeled as significant) was calculated using the SPM extension "CorrClusTh.m" and the Newton-Raphson search method (script provided by Thomas Nichols, University of Warwick, United Kingdom, and Marko Wilke, University of Tübingen, Germany; http://www2.warwick.ac.uk/fac/sci/statistics/staff/academic-research/nichols/scripts/spm/). Anatomical nomenclature for all tables was obtained from the Laboratory for Neuro Imaging (LONI) Brain Atlas (LBPA40, http://www.loni.usc.edu/atlases/; Shattuck et al., 2008).

2.7.5. Connectivity during resting-state periods

Second, we performed linear regression to identify the whole-brain functional connectivity profile of each seed during resting-state. To this end, we extracted the first eigenvector of each seeds' time course. This time course was regressed against all other voxel time courses in the brain, resulting in a seed-specific connectivity map for the baseline, as well as for both post-encoding rest periods. Connectivity maps from the two post-encoding rest periods (i.e., one per study-rest-test cycle) were averaged. Next, we created difference maps (post-encoding minus baseline rest) which were then submitted to a second-level analysis.

To test if connectivity increases from baseline to post-encoding rest were related to durable memory consolidation, we performed a multiple linear regression and added individual memory durability scores as a covariate of interest (see Section 2.3). We repeated this analysis in a separate control step but added general memory performance scores as a covariate of interest. As above, significance was assessed using cluster-inference with a cluster-defining threshold of $p < 0.001$ and a cluster-

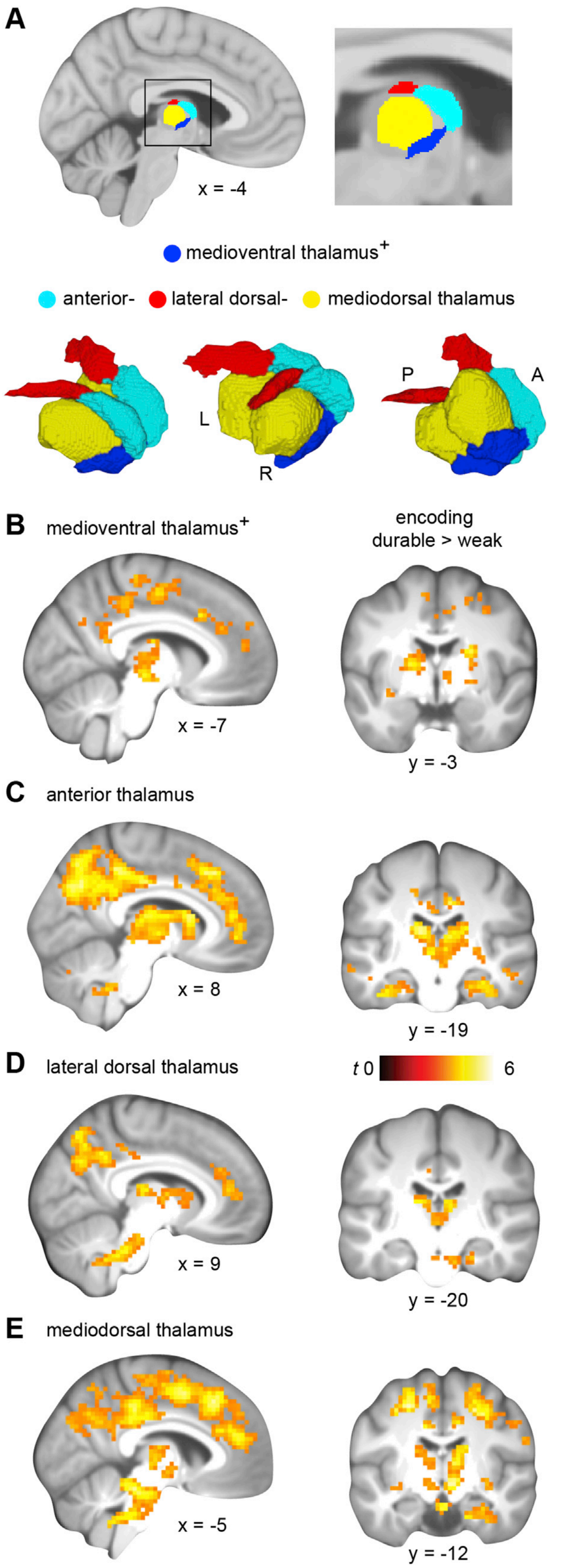

(caption on next column)

Fig. 2. Thalamic regions-of-interest and connectivity increases during durable memory encoding. **(A)** The medioventral thalamus$^+$ (blue), anterior thalamus (cyan), lateral dorsal thalamus (red), and mediodorsal thalamus (yellow). Slices for all figures are based on a mean structural scan. The magnified image (right part) shows the inset as marked on the sagittal brain slice. The lower part shows 3D-renderings of the four thalamic regions. Connectivity from the **(B)** medioventral thalamus$^+$, **(C)** anterior-, **(D)** lateral dorsal-, and **(E)** mediodorsal thalamus during durable compared to weak memory encoding (durable > weak). Results are shown at $p < 0.001$ ($p < 0.05$, FWE-corrected at cluster-level; Table 1). A, anterior; P posterior; L, left; R, right.

probability of $p < 0.05$ FWE-corrected for multiple comparisons.

2.7.6. Activation changes during memory encoding

Following this, we tested if the hypothesized effects were associated with interactions between brain regions rather than to changes in activation levels within thalamic ROIs. For group analysis of activation changes during encoding, contrast images (see Section 2.7.2.) were entered into a second-level random-effects one-way ANOVA with memory durability (forgotten, weak, durable) as within-subject factor. Conditions were compared using post-hoc paired-sample *t*-tests. Again, significance was assessed using cluster-inference with a cluster-defining threshold of $p < 0.001$ and a cluster-probability of $p < 0.05$ FWE-corrected for multiple comparisons. Whole-brain activation levels during encoding (main effect of encoding, durable > forgotten, durable > weak) were reported previously (Wagner et al., 2016). For visualization purposes, we show the whole-brain results (durable > weak, remembered > forgotten) but explicitly focus on encoding-related activation within the thalamic ROIs.

2.7.7. Activation changes and connectivity during memory retrieval

Finally, to test whether our results were related to initial memory formation during encoding and consolidation rather than to retrieval, we also investigated activation changes and connectivity during memory retrieval. fMRI data from the immediate test (day 1) was processed separately from the encoding data. Trials were modeled from trial onset until a button press occurred (i.e., the trial duration equaled the reaction time). All remaining steps were performed identically to the analysis of the encoding data (see Section 2.7.2.).

We used PPI analysis to test whether thalamo-cortical coupling contributed not only to durable memory formation, but also to memory retrieval. Analysis of fMRI data during memory retrieval was performed similar to the analysis during memory encoding (see Section 2.7.4.). In brief, PPIs were calculated per seed region to target durable, as well as general memory encoding (contrasts durable > weak, and remembered > forgotten, respectively). In order to test for group effects, individual contrast images were submitted to one-sample *t*-tests.

Lastly, similar to the activation analysis of the encoding data (see Section 2.7.6.), contrast images from memory retrieval were entered into a second-level random-effects one-way ANOVA with memory durability (forgotten, weak, durable) as within-subject factor. Conditions were compared using post-hoc paired-sample *t*-tests. Whole-brain activation levels during retrieval (main effect of retrieval, durable > forgotten, durable > weak) were reported previously (Wagner et al., 2016). For visualization purposes, we show the whole-brain results (durable > weak, remembered > forgotten) but explicitly focus on retrieval-related activation within the thalamic ROIs. Significance for connectivity and activation results was assessed using cluster-inference with a cluster-defining threshold of $p < 0.001$ and a cluster-probability of $p < 0.05$ FWE-corrected for multiple comparisons.

2.8. Data and code availability statement

All anonymized data and analysis code are available upon request in accordance with the requirements of the institute, the funding body, and the institutional ethics board.

3. Results

3.1. Memory performance and durability scores

Memory performance for both weak and durable associations was above chance level (129.5 remembered associations/4 locations = chance level = 32; number of associations, mean ± SEM: weak: 41.8 ± 2.2, $t(32) = 4.3$, $p < 0.0005$; i.e. 21.8% out of all 192 associations; durable: 87.7 ± 6.5, $t(32) = 8.5$, $p < 0.0005$; i.e. 45.7% out of all 192 associations) (see also Wagner et al., 2016). Approximately one third of the associations were forgotten (60 ± 5.4; 31.3%). The number of weak and durable associations per subject are shown in Fig. 1D (upper part). Interestingly, although the amount of durable memories varied widely, the number of weak memories appeared more or less constant across subjects. Thus, better memory performance was mainly associated with more durable memories.

To investigate resting-state connectivity profiles that were related to durable memory consolidation, we calculated a behavioral "memory durability score" for each subject (see Section 2.3.). Taking into account individual variations in general memory performance (i.e. the total number of remembered associations per subject), approximately 64.9 ± 0.03% of initially remembered associations were also remembered at the delayed test and were thus considered durable. The distribution of individual memory scores is shown in Fig. 1D (lower part). As can be seen, individual memory durability scores ranged from ~32% to ~91% and thus yielded the desirable variance for testing individual differences in durable memory consolidation.

3.2. Thalamo-cortical connectivity increases promote durable memory encoding

As a first step, we hypothesized that thalamo-cortical connectivity of the medioventral thalamus, anterior-, lateral dorsal-, and mediodorsal thalamus would be associated with durable memory formation during encoding. To this end, we investigated thalamic connectivity of the four seed regions (Fig. 2A) using PPI analysis on data obtained during study (see Section 2.7.4.).

Results revealed increased functional coupling of the medioventral thalamus^{+} with surrounding thalamic and striatal regions, the anterior MTL and brainstem, prefrontal and posterior medial structures, left frontal and parietal regions, as well as with the bilateral primary motor cortex during durable compared to weak memory encoding (durable > weak; Fig. 2B, Table 1). Similarly, the anterior-, lateral dorsal-, and mediodorsal thalamus showed increased functional coupling with the surrounding thalamic structures, the hippocampus and adjacent MTL regions, anterior cingulate cortex, MPFC and posterior cingulate cortex (PCC), precuneus, and the brainstem (anterior thalamus, Fig. 2C; lateral dorsal thalamus, Fig. 2D; mediodorsal thalamus, Fig. 2E; all reported in Table 1). Thus, all thalamic seeds displayed increased connectivity with a network that comprised the MTL, MPFC, and the PCC during durable compared to weak memory encoding. We did not find significant connectivity increases for weak compared to durable memory encoding (weak > durable) for any of the seed regions. Also, there were no significant increases in connectivity during encoding of later remembered compared to forgotten associations for any of the seed regions.

Overall, the medioventral thalamus^{+}, anterior-, lateral dorsal-, and mediodorsal thalamus showed increased functional coupling with the MTL, prefrontal and posterior medial structures during durable compared to weak memory encoding, but not during general memory encoding.

3.3. Thalamo-cortical connectivity increases from baseline to post-encoding rest are associated with individual memory durability

Next, we hypothesized that thalamo-cortical connectivity, specifically of the medioventral thalamus, would promote durable memory formation during consolidation after learning. We thus placed a seed within the medioventral thalamus^{+} and investigated thalamo-cortical connectivity increases from baseline to post-encoding rest in relation to individual variations in memory durability (see Section 2.7.5.). Further, we also assessed the contributions of anterior-, lateral dorsal-, and mediodorsal thalamus to durable memory consolidation.

Results showed connectivity increases from baseline rest to post-encoding rest between the medioventral thalamus^{+} and the right posterior parietal cortex and PCC/precuneus, as well as the right superior prefrontal cortex (Fig. 3A, Table 2). The lateral dorsal thalamus was the only other thalamic seed region that showed significant connectivity increases from baseline to post-encoding rest that were positively related to durable memory consolidation. This included enhanced connectivity with bilateral inferior temporal regions, right posterior parietal cortex, PCC and adjacent retrosplenial cortex, as well as with the MPFC (Fig. 3B, Table 2). There was no significant negative relationship between connectivity and individual memory durability scores, and no relationship of connectivity with a *general* memory performance score (i.e., the proportion of remembered associations out of the total number of associations). We did not find any significant connectivity increases associated with memory durability or general memory performance for the anterior and mediodorsal thalamus seeds.

Thus, results showed that significant thalamo-cortical connectivity increases from baseline to post-encoding rest were associated with higher individual memory durability. Specifically, the medioventral and lateral dorsal thalamus showed increased coupling with posterior parietal and posterior medial cortex. The lateral dorsal thalamus revealed additional coupling with inferior temporal regions, retrosplenial cortex, and MPFC.

Table 1
Thalamo-cortical connectivity increases during durable memory encoding (durable > weak). MNI coordinates represent the location of peak voxels. We report the first local maximum within each cluster. Effects were tested for significance using cluster inference with a cluster-defining threshold of $p < 0.001$ and a cluster probability of $p < 0.05$, FWE-corrected for multiple comparisons (critical cluster sizes: medioventral thalamus^{+} seed, 70 voxels; anterior thalamus seed, 77 voxels; lateral dorsal thalamus seed, 80 voxels; mediodorsal thalamus seed, 69 voxels). L, left, R, right.

Seeds and brain regions	MNI coordinates			z-value	cluster size
	x	y	z		
Medioventral thalamus^{+} seed					
brainstem	6	−18	−3	4.91	901
L superior frontal gyrus	−12	18	33	4.54	79
R precentral gyrus	36	−18	54	4.51	664
L middle frontal gyrus	−15	51	36	4.21	148
L middle frontal gyrus	−33	33	48	4.15	104
L precentral gyrus	−24	−15	60	3.97	269
L angular gyrus	−48	−69	18	3.96	137
Anterior thalamus seed					
L lateral orbitofrontal gyrus	−30	21	−9	5.29	5948
Cerebellum	36	−57	−33	4.64	208
Cerebellum	−36	−48	−39	4.53	119
R superior frontal gyrus	9	30	42	4.48	569
R middle frontal gyrus	36	9	36	4.45	405
R fusiform gyrus	39	−24	−24	4.43	201
L parahippocampal gyrus	−33	−12	−27	4.32	143
Brainstem	3	−36	−39	4.21	200
L precentral gyrus	−42	0	39	4.04	137
Lateral dorsal thalamus seed					
Cerebellum	27	−45	−33	4.92	707
L thalamus	−12	−24	15	4.54	396
R superior parietal gyrus	30	−60	42	4.37	1017
R superior frontal gyrus	3	48	9	3.76	156
Mediodorsal thalamus seed					
R superior frontal gyrus	21	9	48	5.15	8696
L middle frontal gyrus	−30	51	15	4.3	163
R superior temporal gyrus	48	−24	12	3.71	118

3.4. Activation during memory encoding

Similar to thalamo-cortical coupling, changes in thalamic activation

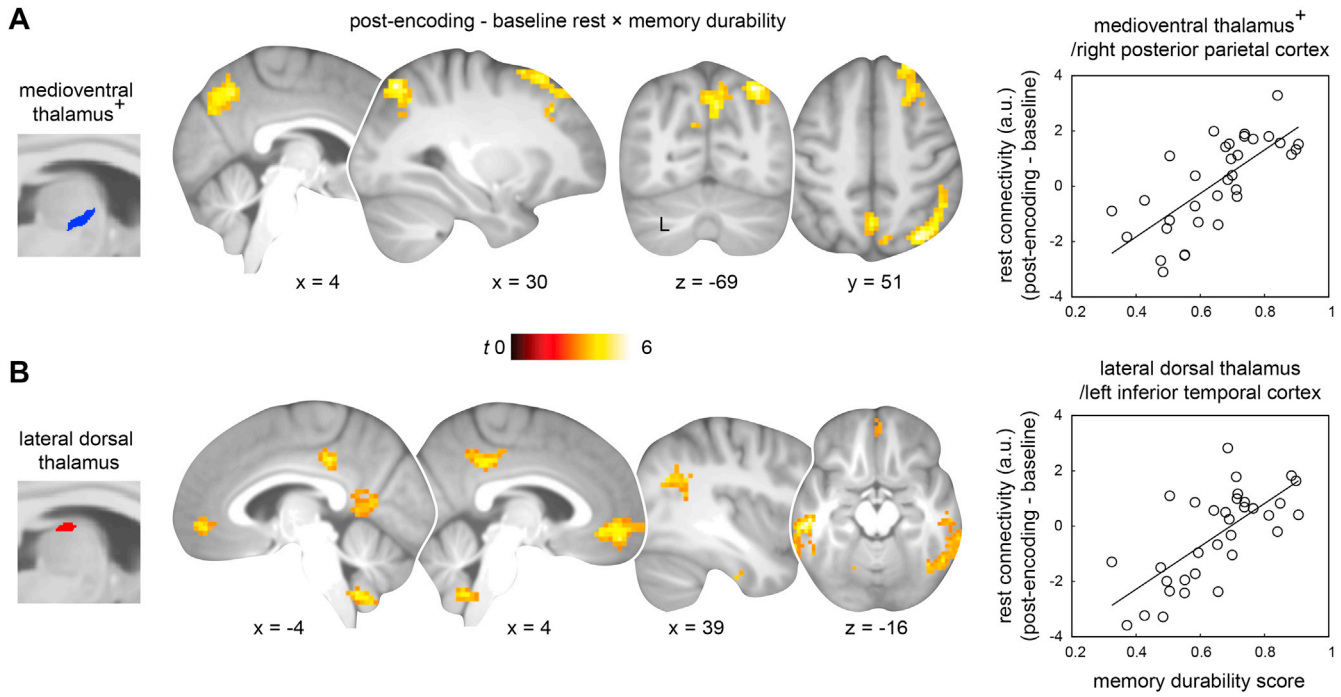

Fig. 3. Thalamo-cortical connectivity increases from baseline to post-encoding rest are associated with individual memory durability. **(A)** Increased medioventral thalamus^{+} connectivity, and **(B)** increased lateral dorsal thalamus connectivity from baseline to post-encoding was positively associated with individual memory durability. Results are shown at $p < 0.001$ ($p < 0.05$, FWE-corrected at cluster-level; Table 2). For visualization purposes, scatter plots show the relationship between individual memory durability and connectivity increases during resting-state (post-encoding minus baseline; % signal change, arbitrary units, a.u.), extracted from the first significant clusters (i.e., **(A)**, right posterior parietal cortex, **(B)**, left inferior temporal cortex). L, left.

Table 2
Thalamo-cortical connectivity increases from baseline to post-encoding rest are associated with individual memory durability. MNI coordinates represent the location of peak voxels. We report the first local maximum within each cluster. Effects were tested for significance using cluster inference with a cluster-defining threshold of $p < 0.001$ and a cluster probability of $p < 0.05$, FWE-corrected for multiple comparisons (critical cluster sizes: medioventral thalamus^{+} seed, 58 voxels; lateral dorsal thalamus seed, 47 voxels). L, left, R, right.

Brain regions	MNI coordinates			*z*-value	cluster size
	x	*y*	*z*		
Medioventral thalamus^{+} seed					
R superior parietal gyrus	30	−69	51	4.53	472
R superior frontal gyrus	27	42	51	4.31	159
L middle frontal gyrus	−27	6	60	3.76	60
Lateral dorsal thalamus seed					
L middle temporal gyrus	−57	−27	−15	4.86	157
R cingulate gyrus	6	−36	36	4.67	172
Cerebellum	−12	−45	−45	4.49	119
Cerebellum	9	−90	−39	4.4	78
Cerebellum	−12	−87	−42	4.28	81
R superior frontal gyrus	3	51	−12	4.27	128
L middle frontal gyrus	−36	6	57	4.07	56
R inferior temporal gyrus	51	−18	−30	4.02	240
L cingulate gyrus	−6	−51	9	3.94	66
R middle occipital gyrus	39	−63	27	3.85	111

levels might signal durable memory encoding. Nevertheless, besides the widespread cortical activation profiles that we reported previously (Wagner et al., 2016), we did not find significant activation changes within any of the thalamic ROIs during durable compared to weak memory encoding (durable > weak; also not for weak > durable).

When investigating activation changes during general memory encoding (remembered > forgotten), we found increased activation within a thalamic region, in addition to significantly increased activation levels in the lateral prefrontal and inferior temporal cortex (Fig. 4A, Table 3). The thalamic cluster did not spatially overlap with the medioventral^{+}-, anterior-, or lateral dorsal thalamus, and only party overlapped with the mediodorsal thalamus at its left lateral border, possibly extending into the ventral part of the ventral lateral posterior nucleus (as confirmed with anatomical overlay, not shown here; Fig. 4C). We extracted activation levels from the four thalamic ROIs to visualize that this small overlap with the mediodorsal thalamus did not contribute to the obtained increased thalamic activation levels during general memory encoding (Fig. 4E).

3.5. Connectivity and activation during memory retrieval

So far, we established that thalamo-cortical interactions were associated with memory durability during encoding and post-encoding rest. To assess whether thalamic regions were also engaged during memory retrieval, we tested connectivity (and activation changes) during the immediate test (day 1; Fig. 1A). Since the immediate test provides subjects with another opportunity to encode, results of this analysis might clarify whether thalamic contributions were associated with initial rather than repeated encoding (during the study and immediate test phase, respectively). PPI analyses revealed no significant increases in thalamo-cortical coupling during durable compared to weak memory retrieval for any of the seeds (durable > weak; also not for weak > durable). In a similar vein, there were no significant thalamo-cortical connectivity changes for any of the seeds during general memory retrieval (remembered > forgotten).

Next, we tested activation levels within thalamic ROIs during memory retrieval. Whole-brain activation profiles were reported in our previous study (Wagner et al., 2016). We did not find significant activation changes within any of the thalamic ROIs during durable compared to weak memory retrieval (durable > weak; also not for weak > durable). However, general memory retrieval (remembered > forgotten) was associated with increased activation levels in the thalamus, along with activation changes in lateral prefrontal cortex, inferior temporal and MTL, PCC, and MPFC (Fig. 4B, Table 3). The thalamic cluster was

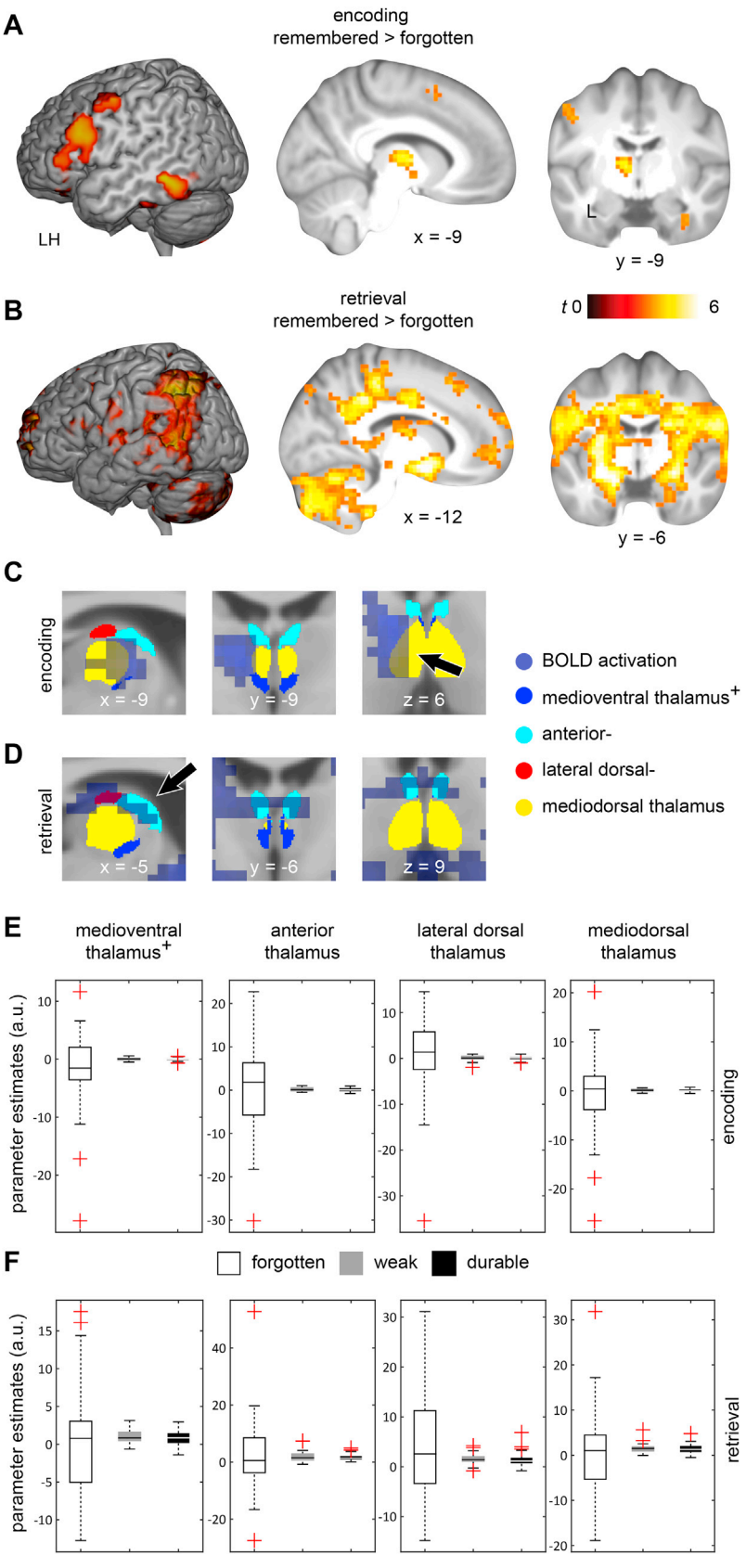

Fig. 4. Thalamo-cortical activation changes during memory encoding and retrieval do not contribute to memory processing. Increased whole-brain BOLD activation during **(A)** encoding and **(B)** retrieval of remembered compared to forgotten associations (remembered > forgotten). Results are shown at $p < 0.001$ ($p < 0.05$, FWE-corrected at cluster-level; Table 3). **(C–D)** Magnified cut-outs show the BOLD activation changes (dark purple, to better appreciate small overlaps) during **(C)** encoding and **(D)** retrieval and their correspondence with thalamic regions (medioventral thalamus^{+}, blue; anterior thalamus, cyan; lateral dorsal thalamus, red; mediodorsal thalamus, yellow). Black arrows indicate the location of overlap of thalamic regions and BOLD activation changes. During encoding, we found increased activation levels that partly overlapped with the mediodorsal thalamus at its left lateral border, but not with medioventral thalamus^{+}, anterior-, or lateral dorsal thalamus. During retrieval, results revealed increased activation within a thalamic cluster that was spatially overlapping with the anterior and lateral dorsal thalamus, but not with the medioventral thalamus^{+} or mediodorsal thalamus. To visualize that these small overlaps did not contribute to the obtained thalamic activation increases during general memory **(E)** encoding and **(F)** retrieval, we extracted activation levels from the respective thalamic ROIs. Box-plots show parameter estimates (arbitrary units, a.u.) per memory durability condition (forgotten, weak, durable). L, left, LH, left hemisphere.

Table 3
Whole-brain activation changes during memory encoding and retrieval (remembered > forgotten). Results (main effect of retrieval, durable > forgotten, durable > weak) were reported previously (Wagner et al., 2016). Here, we explicitly focus on thalamic ROIs but report the whole-brain coordinates of these contrasts (encoding and retrieval, both remembered > forgotten) for completeness. MNI coordinates represent the location of peak voxels. We report the first local maximum within each cluster. Effects were tested for significance using cluster inference with a cluster-defining threshold of $p < 0.001$ and a cluster probability of $p < 0.05$, FWE-corrected for multiple comparisons (critical cluster sizes: memory encoding, 66 voxels; memory retrieval, 65 voxels). L, left, R, right.

Contrasts and brain regions	MNI coordinates			z-value	cluster size
	x	y	z		
Memory encoding					
L inferior temporal gyrus	−48	−51	−12	5.24	595
L thalamus	−9	−9	6	4.75	154
Cerebellum	30	−69	−51	4.7	284
L middle frontal gyrus	−45	18	27	4.62	825
L superior frontal gyrus	−3	12	57	4.61	129
R inferior temporal gyrus	51	−57	−15	4.25	501
Memory retrieval					
L putamen	−15	6	−12	6.64	18091

spatially overlapping with the anterior and lateral dorsal thalamus, but not with the medioventral^{+}- or mediodorsal thalamus (Fig. 4D). For visualization purposes, we again extracted activation levels from the four thalamic ROIs (Fig. 4F). Altogether, neither the medioventral thalamus^{+}, anterior-, lateral dorsal-, or mediodorsal thalamus showed significant functional coupling or activation changes during the retrieval of durable memories.

3.6. Connectivity of the lateral geniculate nucleus during memory processing

To further test the specificity of our results using an independent anatomical region, we analyzed connectivity from the lateral geniculate nucleus (LGN) during memory encoding and consolidation. The LGN forwards visual information from the periphery to the primary visual cortex and plays a role in perception and cognition (O'Connor et al., 2002; Saalmann and Kastner, 2011). We specified the anatomical region by combining the magnocellular and parvocellular LGN masks, collapsed across left and right hemispheres (Krauth et al., 2010), and resliced it to match the dimension of the functional images. The anatomical mask comprised 31 voxels and thus was comparable in size to the anterior thalamus (39 voxels). Again, ROI quality was confirmed through visual inspection of the LGN overlay with subject-specific structural and functional images in MNI standard space. We expected general involvement of the LGN in visual processing and thus no difference in connectivity during durable compared to weak memory encoding, and no consolidation-related connectivity changes. Although the analysis revealed significant LGN coupling with occipital regions during general visual processing (encoding; visual processing > fixation baseline; thus, collapsing across forgotten, weak, and durable memory conditions; Fig. 5; Table 4; retrieval: comparable to results during encoding, not shown in figure but summarized in Table 4), we did not find any significant connectivity changes of the LGN during memory encoding (durable > weak, remembered > forgotten), no significant consolidation-related increased from baseline to post-encoding rest, as well as no significant effects during memory retrieval (durable > weak, remembered > forgotten). Together, this corroborates the specificity of our results in terms of durable memory encoding and consolidation.

4. Discussion

We investigated the role of thalamo-cortical interactions in durable memory formation during initial encoding and consolidation. First, we

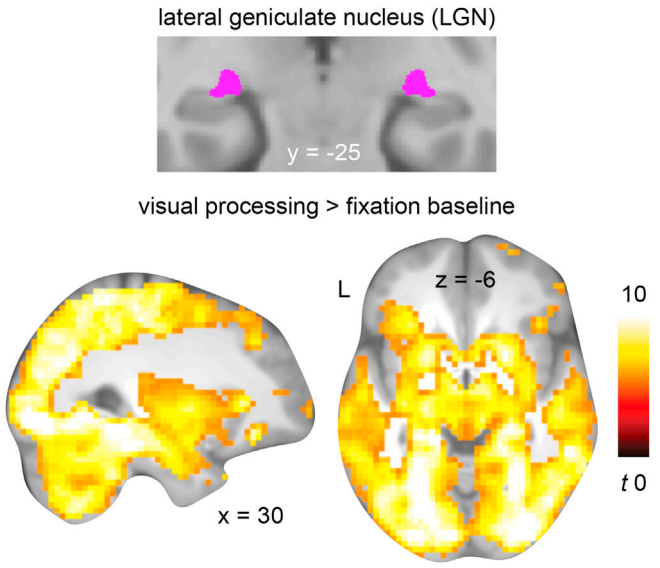

Fig. 5. LGN connectivity increases during visual processing compared to a fixation baseline (encoding task). Results are shown at $p < 0.05$, FWE-corrected for multiple comparisons (Table 4). The PPI during the retrieval task (same contrast) gave comparable results (not shown here but summarized in Table 4). L, left.

Table 4
LGN connectivity increases during visual processing compared to a fixation baseline (visual processing > fixation baseline, during encoding and retrieval tasks). MNI coordinates represent the location of the first 10 peak voxels within the first significant cluster. Effects were thresholded at $p < 0.05$, FWE-corrected for multiple comparisons. L, left, R, right.

Task and brain regions	MNI coordinates			z-value	cluster size
	x	y	z		
Encoding task					
L parahippocampal gyrus	−21	−36	−12	Inf	34666
R inferior occipital gyrus	30	−87	−6	7.7	
Brainstem	−3	−27	−36	7.66	
R postcentral gyrus	42	−24	54	7.57	
R lingual gyrus	27	−57	−3	7.54	
R parahippocampal gyrus	24	−33	−9	7.52	
R inferior temporal gyrus	51	−51	−15	7.39	
L middle occipital gyrus	−27	−90	−9	7.25	
L lingual gyrus	−24	−60	−6	7.23	
Cerebellum	−15	−48	−48	7.2	
Retrieval task					
Cerebellum	18	−75	−30	7.05	30323
R precentral gyrus	21	−27	54	7.01	
R precentral gyrus	54	3	9	7.01	
L superior parietal gyrus	−39	−45	54	6.93	
R superior frontal gyrus	6	6	60	6.87	
L inferior frontal gyrus	−39	24	3	6.86	
Thalamus	6	−9	−3	6.84	
L superior temporal gyrus	−60	−39	3	6.8	
R superior temporal gyrus	63	−9	6	6.78	
L superior frontal gyrus	−6	−15	48	6.77	

found that the medioventral thalamus, as well as the anterior-, lateral dorsal-, and mediodorsal thalamus showed increased neocortical coupling at durable compared to weak memory encoding. Due to the small size of the medioventral thalamus, we also included the adjacent central medial nucleus to form an enlarged seed and thus referred to it as medioventral thalamus^{+}. Second, results revealed significant thalamo-cortical connectivity increases from baseline to post-encoding rest that were associated with higher individual memory durability. More specifically, the medioventral and lateral dorsal thalamus showed increased consolidation-related coupling with posterior parietal and posterior medial cortex. The lateral dorsal thalamus revealed additional coupling

with inferior temporal regions, retrosplenial cortex, and MPFC. Our results were related to durable memory formation, to thalamo-cortical connectivity rather than activation, and to initial memory formation during encoding and consolidation. Furthermore, results were specific to the four thalamic seeds as we did not find significant connectivity of the lateral geniculate nucleus (LGN) during durable compared to weak memory encoding, consolidation, or retrieval.

We expected that increased thalamo-cortical connectivity of the medioventral thalamus would be associated with durable memory formation during encoding. Indeed, we found increased functional coupling between the medioventral thalamus^{+} and the (anterior) MTL, MPFC, and PCC during durable compared to weak memory encoding (Fig. 2B). This connectivity profile was not specific to the medioventral thalamus^{+} but was paralleled by connectivity patterns of adjacent anterior-, lateral dorsal-, and mediodorsal thalamic structures (Fig. 2C–E). The results are in line with previous literature reporting a role of the medioventral thalamus (i.e., the rat nucleus reuniens; Barker and Warburton, 2018), anterior- (Aggleton et al., 1996; Sweeney-Reed et al., 2014, 2015, 2016), lateral dorsal- (Mizumori et al., 1994; Warburton et al., 1997; van Groen et al., 2002), and mediodorsal thalamus (Mitchell and Gaffan, 2008; Pergola et al., 2013; Sweeney-Reed et al., 2016) in (spatial) memory formation. The anterior thalamus is thought to support attentional processes at encoding (Wright et al., 2015; Leszczyński and Staudigl, 2016) and, in addition to the rodent midline thalamus, appears to coordinate the communication along a hippocampal-thalamic-neocortical axis (Aggleton and Brown, 1999; Aggleton et al., 2016). Moreover, successful memory encoding typically engages the medial (Wagner et al., 2016) and lateral prefrontal cortex (Blumenfeld and Ranganath, 2007), and neocortical interactions with these structures might be promoted by the mediodorsal thalamus (Klein et al., 2010; Parnaudeau et al., 2013, 2015). Thus, the medioventral-, anterior-, lateral dorsal-, and mediodorsal thalamus (but not the LGN) appear to interact with neocortical networks to promote durable memory formation at encoding. Future studies might try to disentangle the exact, encoding-related roles of these thalamic subregions.

Next, we asked whether thalamo-cortical coupling would be associated with durable memory formation during consolidation after learning. Results demonstrated connectivity increases from baseline to post-encoding rest between the medioventral^{+}- and lateral dorsal thalamus with the right posterior parietal cortex that were associated with higher individual memory durability across subjects (Fig. 3). We suggest that the posterior parietal cortex coded for the specific locations of the previously studied pictures, as it has been implicated in the representation of picture-location associations (Takashima et al., 2007), egocentric spatial content (Burgess et al., 2001), and the retinotopic angle of remembered target locations (Sereno et al., 2001). Both seeds were further coupled with the PCC/precuneus (Fig. 3), and the lateral dorsal thalamus showed additional connectivity with the MPFC and inferior temporal regions, altogether positively scaling with individual memory durability across subjects (Fig. 3B). The MPFC and PCC are regarded as central for successful memory encoding (PCC: Daselaar et al., 2004, 2009; Huijbers et al., 2012; MPFC and PCC: Wagner et al., 2016), consolidation (MPFC: Takashima et al., 2009; van Kesteren et al., 2010; Schlichting and Preston, 2015; PCC: Kaplan et al., 2016), and retrieval (MPFC and PCC: Takashima et al., 2007; Rugg and Vilberg, 2012; King et al., 2015; Wagner et al., 2015, 2016). Lateral dorsal thalamic connectivity with the MPFC and PCC during post-encoding rest therefore likely reflected the consolidation of memory traces into durable engrams. Additionally, we suggest that the inferior temporal cortex coded for the specific content of the previously learned picture-location associations. Thalamic connectivity to the posterior parietal and inferior temporal cortex might thus strengthen mnemonic representations of the studied associations (Tambini et al., 2010; van Kesteren et al., 2010; Schlichting and Preston, 2014). This is specific to the task material at hand and other representational regions might be involved in the consolidation of different stimulus material. Altogether, these results appeared specific for the medioventral thalamus^{+} and lateral dorsal thalamus as we did not find significant consolidation-related coupling of the anterior and mediodorsal thalamus, or the LGN.

Memory consolidation during awake rest or sleep has been associated with reactivation of neuronal ensembles that were engaged during preceding experiences (Wilson and McNaughton, 1994; Carr et al., 2011). Such "replay" often coincides with high-frequency bursts in neuronal firing, so-called sharp-wave ripples, that are thought to establish hippocampal communication with neocortical regions (Girardeau et al., 2009; Jadhav et al., 2012; Logothetis et al., 2012), including the PCC (Kaplan et al., 2016) and MPFC (Euston et al., 2007; Peyrache et al., 2009). Notably, such cortical interactions are mediated by the thalamus (Guillery and Sherman, 2002; Sherman and Guillery, 2002; Sherman, 2005, 2007, 2016). For instance, Logothetis et al. (2012) identified sharp-wave ripples during resting-state in primates and measured BOLD changes time-locked to their onset. Most of the cortex was activated during ripples, whereas thalamic regions showed BOLD suppression. This was interpreted as thalamic orchestration of hippocampal-neocortical interactions. Signal suppression might temporarily block sensory processing and so promote interference-free consolidation (see also Yang et al., 2019). In line with this, we suggest that the thalamo-cortical networks at issue here facilitates durable memory consolidation after learning.

Consolidation is thought to downscale hippocampal contributions and to bolster neocortical interactions, eventually leading to enhanced MPFC engagement (Marr, 1970; Frankland and Bontempi, 2005; Takashima et al., 2006; Takehara-Nishiuchi and McNaughton, 2008). These interactions are thought to be relayed via the rat nucleus reuniens (i.e., the medioventral thalamus in humans) as it links the structural pathways of hippocampus and MPFC (Vertes et al., 2007). Surprisingly, we did not find any significant increases in consolidation-related coupling between the medioventral thalamus and hippocampus or MPFC during post-encoding rest (although we did find lateral dorsal thalamus-MPFC connectivity). Consolidation is thought to follow initial encoding and so contribute to memory formation but the line between these processes is artificial and it can probably not be determined when encoding ends and when consolidation begins. The interplay between regions at the level of connectivity and/or activation might be different during encoding and consolidation. Indeed, we found elevated consolidation-related connectivity between the medioventral thalamus, MTL and MPFC at durable memory encoding (Fig. 2B). Thalamo-cortical coupling might determine the formation of durable memories as they are initially processed, and interactions between the medioventral- and lateral dorsal thalamus with posterior representational regions might further boost consolidation thereafter.

Durable memories are assumed to be encoded by distributed, neocortical networks (Marr, 1970; Frankland and Bontempi, 2005). For example, Wheeler et al. (2013) investigated the functional connectome of a long-term fear memory trace in mice (Wheeler et al., 2013). The authors demonstrated that the memory trace depended on a widespread network centered on the nucleus reuniens (i.e., the human medioventral thalamus), hippocampus, MPFC, and neocortical structures. Similarly, Thielen and colleagues (2015) found that memory traces were associated with a distributed set of regions, comprising the thalamus, the hippocampus, MPFC, and posterior representational regions. Our findings align with these reports as we found that thalamo-cortical interactions rather than activation changes within thalamic regions supported memory encoding and consolidation. Furthermore, our results were associated with durable rather than general memory formation, and we did not find significant thalamo-cortical engagement during memory retrieval. The thalamus might therefore constitute a central node within a broad, neocortical network that specifically supports the formation of durable memories.

Several limitations need to be addressed. First, due to the small size of the medioventral thalamus, we combined it with the adjacent central medial nucleus to form an appropriate seed region for our analyses. The rodent central medial nucleus receives its main input from the brainstem

and other subcortical structures and in turn exhibits widespread projections to subcortical and cortical regions, including the prefrontal cortex, dorsal and ventral striatum, and the amygdala (Vertes et al., 2012). Considering this, significant connectivity between the medioventral thalamus^{+}, striatum, brainstem, and prefrontal cortex might be partly due to the inclusion of the central medial nucleus in the seed (Fig. 2B). Due to its structural connectivity, the central medial nucleus was suggested to play a role in arousal and awareness (Van der Werf et al., 2002), and goal-directed behavior (Vertes et al., 2012), and we speculate that it might also affect durable memory encoding. Second, we used the thalamic atlas by Krauth et al. (2010) which is based on data from a small subject sample. Differences in individual anatomy might be associated with anatomical imprecision and reference frames based on larger samples could ameliorate this issue in future studies. Third, our image resolution of 3 mm (and subsequent smoothing with 6 mm) might have mixed signals from neighboring thalamic seeds. To fully resolve this issue, we recommend that future studies should employ high resolution imaging. Relatedly, although we did not find significant effects of thalamic connectivity during memory retrieval, we cannot rule out possible contributions of specific thalamic subregions within the medioventral thalamus^{+}, anterior-, lateral dorsal-, or mediodorsal thalamus to retrieval (see also Pergola et al., 2013). The regions-of-interest that we included might have been substantially larger than the neuronal representation actually involved. Despite these constraints, we present novel, exploratory findings that implicate thalamo-cortical interactions in durable memory encoding and consolidation.

5. Conclusions

To conclude, we showed that increased coupling of a thalamic region including the medioventral thalamus (which also comprised the adjacent central medial nucleus), the anterior-, lateral dorsal-, and mediodorsal thalamic structures, with the MTL, anterior and posterior midline regions supported durable memory encoding. Increased consolidated-related interactions of the medioventral thalamus and lateral dorsal thalamus with the PCC and posterior representational regions were associated with the proportion of durable memories that subjects formed. Additionally, the lateral dorsal thalamus exhibited consolidation-related increased with the MPFC. Our results suggest a model in which the thalamus acts as a central node that links hippocampal with neocortical networks during initial, durable memory formation. This thalamic link might decrease over time as consolidation progresses, rendering memories neocortically dependent. Together, we suggest that thalamo-cortical cross-talk strengthens durable memory engrams at initial encoding, and that thalamo-cortical interactions centered on specific thalamic subregions support their consolidation thereafter.

Conflicts of interest

The authors declare no competing financial interests.

Acknowledgements

The authors would like to thank Leonore Bovy for assistance with data acquisition. This project was supported by a grant from the European Research Council (ERC R0001075) to Guillén Fernández.

References

Aggleton, J.P., Brown, M.W., 1999. Episodic memory, amnesia, and the hippocampal-anterior thalamic axis. Behav. Brain Sci. 22, 425–444 discussion 444-89.
Aggleton, J.P., Hunt, P.R., Nagle, S., Neave, N., 1996. The effects of selective lesions within the anterior thalamic nuclei on spatial memory in the rat. Behav. Brain Res. 81, 189–198.
Aggleton, J.P., Nelson, A.J.D., 2015. Why do lesions in the rodent anterior thalamic nuclei cause such severe spatial deficits? Neurosci. Biobehav. Rev. 54, 131–144.
Aggleton, J.P., Pralus, A., Nelson, A.J.D., Hornberger, M., 2016. Thalamic pathology and memory loss in early Alzheimer's disease: moving the focus from the medial temporal lobe to Papez circuit. Brain 139, 1877–1890.
Ashburner, J., 2007. A fast diffeomorphic image registration algorithm. Neuroimage 38, 95–113.
Barker, G.R.I., Warburton, E.C., 2018. A critical role for the nucleus reuniens in long-term, but not short-term associative recognition memory formation. J. Neurosci. 38, 3208–3217.
Birn, R.M., Diamond, J.B., Smith, M.A., Bandettini, P.A., 2006. Separating respiratory-variation-related fluctuations from neuronal-activity-related fluctuations in fMRI. Neuroimage 31, 1536–1548.
Blumenfeld, R.S., Ranganath, C., 2007. Prefrontal cortex and long-term memory encoding: an integrative review of findings from neuropsychology and neuroimaging. Neuroscientist 13, 280–291.
Browning, P.G.F., Chakraborty, S., Mitchell, A.S., 2015. Evidence for mediodorsal thalamus and prefrontal cortex interactions during cognition in macaques. Cerebr. Cortex 25, 4519–4534.
Burgess, N., Becker, S., King, J.A., O'Keefe, J., 2001. Memory for events and their spatial context: models and experiments. Philos. Trans. R. Soc. Lond. B Biol. Sci. 356, 1493–1503.
Carr, M.F., Jadhav, S.P., Frank, L.M., 2011. Hippocampal replay in the awake state: a potential substrate for memory consolidation and retrieval. Nat. Neurosci. 14, 147–153.
Cassel, J.-C., Pereira de Vasconcelos, A., Loureiro, M., Cholvin, T., Dalrymple-Alford, J.C., Vertes, R.P., 2013. The reuniens and rhomboid nuclei: neuroanatomy, electrophysiological characteristics and behavioral implications. Prog. Neurobiol. 111, 34–52.
Cholvin, T., Hok, V., Giorgi, L., Chaillan, F., Poucet, B., 2017. Ventral midline thalamus is necessary for hippocampal place field stability and cell firing modulation. J. Neurosci. 38, 2039–17.
Cross, L., Brown, M.W., Aggleton, J.P., Warburton, E.C., 2012. The medial dorsal thalamic nucleus and the medial prefrontal cortex of the rat function together to support associative recognition and recency but not item recognition. Learn. Mem. 20, 41–50.
Daselaar, S.M., Prince, S.E., Cabeza, R., 2004. When less means more: deactivations during encoding that predict subsequent memory. Neuroimage 23, 921–927.
Daselaar, S.M., Prince, S.E., Dennis, N.A., Hayes, S.M., Kim, H., Cabeza, R., 2009. Posterior midline and ventral parietal activity is associated with retrieval success and encoding failure. Front. Hum. Neurosci. 3, 13.
Davoodi, F.G., Motamedi, F., Akbari, E., Ghanbarian, E., Jila, B., 2011. Effect of reversible inactivation of reuniens nucleus on memory processing in passive avoidance task. Behav. Brain Res. 221, 1–6.
Diekelmann, S., Born, J., 2010. The memory function of sleep. Nat. Rev. Neurosci. 11, 114–126.
Dolleman-Van Der Weel, M.J., Witter, M.P., 1996. Projections from the nucleus reuniens thalami to the entorhinal cortex, hippocampal field CA1, and the subiculum in the rat arise from different populations of neurons. J. Comp. Neurol. 364, 637–650.
Dudai, Y., 2004. The neurobiology of consolidations, or, how stable is the engram? Annu. Rev. Psychol. 55, 51–86.
Euston, D.R., Tatsuno, M., McNaughton, B.L., 2007. Fast-forward playback of recent memory sequences in prefrontal cortex during sleep. Science 318, 1147–1150.
Frankland, P.W., Bontempi, B., 2005. The organization of recent and remote memories. Nat. Rev. Neurosci. 6, 119–130.
Friston, K.J., Buechel, C., Fink, G.R., Morris, J., Rolls, E., Dolan, R.J., 1997. Psychophysiological and modulatory interactions in neuroimaging. Neuroimage 6, 218–229.
Girardeau, G., Benchenane, K., Wiener, S.I., Buzsáki, G., Zugaro, M.B., 2009. Selective suppression of hippocampal ripples impairs spatial memory. Nat. Neurosci. 12, 1222–1223.
Glover, G.H., Li, T.Q., Ress, D., 2000. Image-based method for retrospective correction of physiological motion effects in fMRI: RETROICOR. Magn. Reson. Med. 44, 162–167.
Grill-Spector, K., Weiner, K.S., 2014. The functional architecture of the ventral temporal cortex and its role in categorization. Nat. Rev. Neurosci. 15, 536–548.
Guillery, R.W., Sherman, S.M., 2002. Thalamic relay functions and their role in corticocortical communication. Neuron 33, 163–175.
Hoover, W.B., Vertes, R.P., 2007. Anatomical analysis of afferent projections to the medial prefrontal cortex in the rat. Brain Struct. Funct. 212, 149–179.
Hoover, W.B., Vertes, R.P., 2012. Collateral projections from nucleus reuniens of thalamus to hippocampus and medial prefrontal cortex in the rat: a single and double retrograde fluorescent labeling study. Brain Struct. Funct. 217, 191–209.
Huijbers, W., Vannini, P., Sperling, R.A., C M P, Cabeza, R., Daselaar, S.M., 2012. Explaining the encoding/retrieval flip: memory-related deactivations and activations in the posteromedial cortex. Neuropsychologia 50, 3764–3774.
Jadhav, S.P., Kemere, C., German, P.W., Frank, L.M., 2012. Awake hippocampal sharp-wave ripples support spatial memory. Science 336, 1454–1458.
Jay, T.M., Glowinski, J., Thierry, A.M., 1989. Selectivity of the hippocampal projection to the prelimbic area of the prefrontal cortex in the rat. Brain Res. 505, 337–340.
Johansen-Berg, H., Behrens, T.E.J., Sillery, E., Ciccarelli, O., Thompson, A.J., Smith, S.M., Matthews, P.M., 2005. Functional-anatomical validation and individual variation of diffusion tractography-based segmentation of the human thalamus. Cerebr. Cortex 15, 31–39.
Kaplan, R., Adhikari, M.H., Hindriks, R., Mantini, D., Murayama, Y., Logothetis, N.K., Deco, G., 2016. Hippocampal sharp-wave ripples influence selective activation of the default mode network. Curr. Biol. 26, 686–691.
Ketz, N.A., Jensen, O., O'Reilly, R.C., 2015. Thalamic pathways underlying prefrontal cortex–medial temporal lobe oscillatory interactions. Trends Neurosci. 38, 3–12.

King, D.R., de Chastelaine, M., Elward, R.L., Wang, T.H., Rugg, M.D., 2015. Recollection-related increases in functional connectivity predict individual differences in memory accuracy. J. Neurosci. 35, 1763–1772.
Klein, J.C., Rushworth, M.F.S., Behrens, T.E.J., Mackay, C.E., de Crespigny, A.J., D'Arceuil, H., Johansen-Berg, H., 2010. Topography of connections between human prefrontal cortex and mediodorsal thalamus studied with diffusion tractography. Neuroimage 51, 555–564.
Krauth, A., Blanc, R., Poveda, A., Jeanmonod, D., Morel, A., Székely, G., 2010. A mean three-dimensional atlas of the human thalamus: generation from multiple histological data. Neuroimage 49, 2053–2062.
Kriegeskorte, N., Mur, M., Ruff, D.A., Kiani, R., Bodurka, J., Esteky, H., Tanaka, K., Bandettini, P.A., 2008. Matching categorical object representations in inferior temporal cortex of man and monkey. Neuron 60, 1126–1141.
Leszczyński, M., Staudigl, T., 2016. Memory-guided attention in the anterior thalamus. Neurosci. Biobehav. Rev. 66, 163–165.
Logothetis, N.K., Eschenko, O., Murayama, Y., Augath, M., Steudel, T., Evrard, H.C., Besserve, M., Oeltermann, A., 2012. Hippocampal-cortical interaction during periods of subcortical silence. Nature 491, 547–553.
Loureiro, M., Cholvin, T., Lopez, J., Merienne, N., Latreche, A., Cosquer, B., Geiger, K., Kelche, C., Cassel, J.-C., Pereira de Vasconcelos, A., 2012. The ventral midline thalamus (reuniens and rhomboid nuclei) contributes to the persistence of spatial memory in rats. J. Neurosci. 32, 9947–9959.
Maingret, N., Girardeau, G., Todorova, R., Goutierre, M., Zugaro, M., 2016. Hippocampo-cortical coupling mediates memory consolidation during sleep. Nat. Neurosci. 19, 959–964.
Marr, D., 1970. A theory for cerebral neocortex. Proc. R. Soc. Lond. B Biol. Sci. 176, 161–234.
Martin, A., Wiggs, C.L., Ungerleider, L.G., Haxby, J.V., 1996. Neural correlates of category-specific knowledge. Nature 379, 649–652.
Miller, R.L.A., Francoeur, M.J., Gibson, B.M., Mair, R.G., 2017. Mediodorsal thalamic neurons mirror the activity of medial prefrontal neurons responding to movement and reinforcement during a dynamic DNMTP task. eneuro 4. ENEURO.0196-17.2017.
Mitchell, A.S., Gaffan, D., 2008. The magnocellular mediodorsal thalamus is necessary for memory acquisition, but not retrieval. J. Neurosci. 28, 258–263.
Mizumori, S.J., Miya, D.Y., Ward, K.E., 1994. Reversible inactivation of the lateral dorsal thalamus disrupts hippocampal place representation and impairs spatial learning. Brain Res. 644, 168–174.
Mizumori, S.J., Williams, J.D., 1993. Directionally selective mnemonic properties of neurons in the lateral dorsal nucleus of the thalamus of rats. J. Neurosci. 13, 4015–4028.
Morel, A., 2007. Stereotactic atlas of the human thalamus and basal ganglia. CRC Press, Boca Raton.
O'Connor, D.H., Fukui, M.M., Pinsk, M.A., Kastner, S., 2002. Attention modulates responses in the human lateral geniculate nucleus. Nat. Neurosci. 5, 1203–1209.
Parnaudeau, S., O'Neill, P.-K., Bolkan, S.S., Ward, R.D., Abbas, A.I., Roth, B.L., Balsam, P.D., Gordon, J.A., Kellendonk, C., 2013. Inhibition of mediodorsal thalamus disrupts thalamofrontal connectivity and cognition. Neuron 77, 1151–1162.
Parnaudeau, S., Taylor, K., Bolkan, S.S., Ward, R.D., Balsam, P.D., Kellendonk, C., 2015. Mediodorsal thalamus hypofunction impairs flexible goal-directed behavior. Biol. Psychiatry 77, 445–453.
Peigneux, P., Orban, P., Balteau, E., Degueldre, C., Luxen, A., Laureys, S., Maquet, P., 2006. Offline persistence of memory-related cerebral activity during active wakefulness. PLoS Biol. 4, e100.
Pergola, G., Ranft, A., Mathias, K., Suchan, B., 2013. The role of the thalamic nuclei in recognition memory accompanied by recall during encoding and retrieval: an fMRI study. Neuroimage 74, 195–208.
Peyrache, A., Khamassi, M., Benchenane, K., Wiener, S.I., Battaglia, F.P., 2009. Replay of rule-learning related neural patterns in the prefrontal cortex during sleep. Nat. Neurosci. 12, 919–926.
Poser, B.A., Versluis, M.J., Hoogduin, J.M., Norris, D.G., 2006. BOLD contrast sensitivity enhancement and artifact reduction with multiecho EPI: parallel-acquired inhomogeneity-desensitized fMRI. Magn. Reson. Med. 55, 1227–1235.
Power, J.D., Barnes, K.A., Snyder, A.Z., Schlaggar, B.L., Petersen, S.E., 2012. Spurious but systematic correlations in functional connectivity MRI networks arise from subject motion. Neuroimage 59, 2142–2154.
Puelles, L., Martinez-de-la-Torre, M., Ferran, J., Watson, C., 2012. Diencephalon. In: Watson, C., Paxinos, G., Puelles, L. (Eds.), The Mouse Nervous System. Academic Press, pp. 313–336.
Rugg, M.D., Vilberg, K.L., 2012. Brain networks underlying episodic memory retrieval. Curr. Opin. Neurobiol. 23, 255–260.
Saalmann, Y.B., Kastner, S., 2011. Cognitive and perceptual functions of the visual thalamus. Neuron 71, 209–223.
Schlichting, M.L., Preston, A.R., 2014. Memory reactivation during rest supports upcoming learning of related content. Proc. Natl. Acad. Sci. U. S. A. 111, 15845–15850.
Schlichting, M.L., Preston, A.R., 2015. Hippocampal-medial prefrontal circuit supports memory updating during learning and post-encoding rest. Neurobiol. Learn. Mem. 134, 91–106.
Sereno, M.I., Pitzalis, S., Martinez, A., 2001. Mapping of contralateral space in retinotopic coordinates by a parietal cortical area in humans. Science 294, 1350–1354.
Shattuck, D.W., Mirza, M., Adisetiyo, V., Hojatkashani, C., Salamon, G., Narr, K.L., Poldrack, R.A., Bilder, R.M., Toga, A.W., 2008. Construction of a 3D probabilistic atlas of human cortical structures. Neuroimage 39, 1064–1080.
Sherman, S.M., 2005. Thalamic relays and cortical functioning. Prog. Brain Res. 149, 107–126.
Sherman, S.M., 2007. The thalamus is more than just a relay. Curr. Opin. Neurobiol. 17, 417–422.
Sherman, S.M., 2016. Thalamus plays a central role in ongoing cortical functioning. Nat. Neurosci. 16, 533–541.
Sherman, S.M., Guillery, R.W., 2002. The role of the thalamus in the flow of information to the cortex. Philos. Trans. R. Soc. Lond. B Biol. Sci. 357, 1695–1708.
Shmueli, K., van Gelderen, P., de Zwart, J.A., Horovitz, S.G., Fukunaga, M., Jansma, J.M., Duyn, J.H., 2007. Low-frequency fluctuations in the cardiac rate as a source of variance in the resting-state fMRI BOLD signal. Neuroimage 38, 306–320.
Sneve, M.H., Grydeland, H., Nyberg, L., Bowles, B., Amlien, I.K., Langnes, E., Walhovd, K.B., Fjell, A.M., 2015. Mechanisms underlying encoding of short-lived versus durable episodic memories. J. Neurosci. 35, 5202–5212.
Squire, L.R., Genzel, L., Wixted, J.T., Morris, R.G., 2015. Memory consolidation. Cold Spring Harbor Perspect. Biol. 7, a021766.
Stickgold, R., Walker, M.P., 2013. Sleep-dependent memory triage: evolving generalization through selective processing. Nat. Neurosci. 16, 139–145.
Sweeney-Reed, C.M., Zaehle, T., Voges, J., Schmitt, F.C., Buentjen, L., Kopitzki, K., Esslinger, C., Hinrichs, H., Heinze, H.-J., Knight, R.T., Richardson-Klavehn, A., 2014. Corticothalamic phase synchrony and cross-frequency coupling predict human memory formation. Elife 3, e05352.
Sweeney-Reed, C.M., Zaehle, T., Voges, J., Schmitt, F.C., Buentjen, L., Kopitzki, K., Hinrichs, H., Heinze, H.-J., Rugg, M.D., Knight, R.T., Richardson-Klavehn, A., 2015. Thalamic theta phase alignment predicts human memory formation and anterior thalamic cross-frequency coupling. Elife 4.
Sweeney-Reed, C.M., Zaehle, T., Voges, J., Schmitt, F.C., Buentjen, L., Kopitzki, K., Richardson-Klavehn, A., Hinrichs, H., Heinze, H.-J., Knight, R.T., Rugg, M.D., 2016. Pre-stimulus thalamic theta power predicts human memory formation. Neuroimage 138, 100–108.
Takashima, A., Nieuwenhuis, I.L.C., Jensen, O., Talamini, L.M., Rijpkema, M., Fernández, G., 2009. Shift from hippocampal to neocortical centered retrieval network with consolidation. J. Neurosci. 29, 10087–10093.
Takashima, A., Nieuwenhuis, I.L.C., Rijpkema, M., Petersson, K.M., Jensen, O., Fernández, G., 2007. Memory trace stabilization leads to large-scale changes in the retrieval network: a functional MRI study on associative memory. Learn. Mem. 14, 472–479.
Takashima, A., Petersson, K.M., Rutters, F., Tendolkar, I., Jensen, O., Zwarts, M.J., McNaughton, B.L., Fernandez, G., 2006. Declarative memory consolidation in humans: a prospective functional magnetic resonance imaging study. Proc. Natl. Acad. Sci. U. S. A. 103, 756–761.
Takehara-Nishiuchi, K., McNaughton, B.L., 2008. Spontaneous changes of neocortical code for associative memory during consolidation. Science 80 (322), 960–963.
Tambini, A., Ketz, N., Davachi, L., 2010. Enhanced brain correlations during rest are related to memory for recent experiences. Neuron 65, 280–290.
Taube, J.S., 1995. Head direction cells recorded in the anterior thalamic nuclei of freely moving rats. J. Neurosci. 15, 70–86.
van Buuren, M., Gladwin, T.E., Zandbelt, B.B., van den Heuvel, M., Ramsey, N.F., Kahn, R.S., Vink, M., 2009. Cardiorespiratory effects on default-mode network activity as measured with fMRI. Hum. Brain Mapp. 30, 3031–3042.
van Buuren, M., Kroes, M.C.W., Wagner, I.C., Genzel, L., Morris, R.G.M., Fernández, G., 2014. Initial investigation of the effects of an experimentally learned schema on spatial associative memory in humans. J. Neurosci. 34, 16662–16670.
Van der Werf, Y.D., Witter, M.P., Groenewegen, H.J., 2002. The intralaminar and midline nuclei of the thalamus. Anatomical and functional evidence for participation in processes of arousal and awareness. Brain Res. Rev. 39, 107–140.
van Dongen, E.V., Takashima, A., Barth, M., Fernández, G., 2011. Functional connectivity during light sleep is correlated with memory performance for face-location associations. Neuroimage 57, 262–270.
van Dongen, E.V., Thielen, J.-W., Takashima, A., Barth, M., Fernández, G., 2012. Sleep supports selective retention of associative memories based on relevance for future utilization. PLoS One 7, e43426.
van Groen, T., Kadish, I., Wyss, J.M., 2002. The role of the laterodorsal nucleus of the thalamus in spatial learning and memory in the rat. Behav. Brain Res. 136, 329–337.
van Kesteren, M.T.R., Fernández, G., Norris, D.G., Hermans, E.J., 2010. Persistent schema-dependent hippocampal-neocortical connectivity during memory encoding and postencoding rest in humans. Proc. Natl. Acad. Sci. U. S. A. 107, 7550–7555.
Varela, C., Kumar, S., Yang, J.Y., Wilson, M.A., 2014. Anatomical substrates for direct interactions between hippocampus, medial prefrontal cortex, and the thalamic nucleus reuniens. Brain Struct. Funct. 219, 911–929.
Vertes, R.P., 2002. Analysis of projections from the medial prefrontal cortex to the thalamus in the rat, with emphasis on nucleus reuniens. J. Comp. Neurol. 442, 163–187.
Vertes, R.P., 2004. Differential projections of the infralimbic and prelimbic cortex in the rat. Synapse 51, 32–58.
Vertes, R.P., 2006. Interactions among the medial prefrontal cortex, hippocampus and midline thalamus in emotional and cognitive processing in the rat. Neuroscience 142, 1–20.
Vertes, R.P., Hoover, W.B., Rodriguez, J.J., 2012. Projections of the central medial nucleus of the thalamus in the rat: node in cortical, striatal and limbic forebrain circuitry. Neuroscience 219, 120–136.
Vertes, R.P., Hoover, W.B., Szigeti-Buck, K., Leranth, C., 2007. Nucleus reuniens of the midline thalamus: link between the medial prefrontal cortex and the hippocampus. Brain Res. Bull. 71, 601–609.
Wagner, I.C., van Buuren, M., Bovy, L., Fernandez, G., 2016. Parallel engagement of regions associated with encoding and later retrieval forms durable memories. J. Neurosci. 36, 7985–7995.

Wagner, I.C., van Buuren, M., Bovy, L., Morris, R.G., Fernández, G., 2017. Methylphenidate during early consolidation affects long-term associative memory retrieval depending on baseline catecholamines. Psychopharmacology (Berlin) 234, 657–669.
Wagner, I.C., van Buuren, M., Kroes, M.C., Gutteling, T.P., van der Linden, M., Morris, R.G., Fernández, G., 2015. Schematic memory components converge within angular gyrus during retrieval. Elife 4.
Warburton, E.C., Baird, A.L., Aggleton, J.P., 1997. Assessing the magnitude of the allocentric spatial deficit associated with complete loss of the anterior thalamic nuclei in rats. Behav. Brain Res. 87, 223–232.
Wheeler, A.L., Teixeira, C.M., Wang, A.H., Xiong, X., Kovacevic, N., Lerch, J.P., McIntosh, A.R., Parkinson, J., Frankland, P.W., 2013. Identification of a functional connectome for long-term fear memory in mice. PLoS Comput. Biol. 9, e1002853.
Wilson, M.A., McNaughton, B.L., 1994. Reactivation of hippocampal ensemble memories during sleep. Science 265, 676–679.
Wright, N.F., Vann, S.D., Aggleton, J.P., Nelson, A.J.D., 2015. A critical role for the anterior thalamus in directing attention to task-relevant stimuli. J. Neurosci. 35, 5480–5488.
Xu, W., Südhof, T.C., 2013. A neural circuit for memory specificity and generalization. Science 339, 1290–1295.
Yang, M., Logothetis, N.K., Eschenko, O., 2019. Occurrence of hippocampal ripples is associated with activity suppression in the mediodorsal thalamic nucleus. J. Neurosci. 39, 434–444.